



OPEN ACCESS

EDITED BY

João Canário,
University of Lisbon, Portugal

REVIEWED BY

Carlos Eduardo Monteiro,
IST-ID, Portugal
Chao Song,
Shandong University, China
Manuel David Montaña,
Western Washington University, United States

*CORRESPONDENCE

Subhasis Ghoshal,
✉ subhasis.ghoshal@mcgill.ca

RECEIVED 15 October 2024

ACCEPTED 20 January 2025

PUBLISHED 27 February 2025

CITATION

Rao S, Gao X and Ghoshal S (2025)
Characterization of the fate of primary and re-precipitated silver nanoparticles in lake water model systems.
Front. Environ. Chem. 6:1511440.
doi: 10.3389/fenvc.2025.1511440

COPYRIGHT

© 2025 Rao, Gao and Ghoshal. This is an open-access article distributed under the terms of the [Creative Commons Attribution License \(CC BY\)](https://creativecommons.org/licenses/by/4.0/). The use, distribution or reproduction in other forums is permitted, provided the original author(s) and the copyright owner(s) are credited and that the original publication in this journal is cited, in accordance with accepted academic practice. No use, distribution or reproduction is permitted which does not comply with these terms.

Characterization of the fate of primary and re-precipitated silver nanoparticles in lake water model systems

Sarayu Rao¹, Xiaoyu Gao^{1,2} and Subhasis Ghoshal^{1*}

¹Department of Civil Engineering, McGill University, Montreal, QC, Canada, ²Department of Environmental Science, Baylor University, Waco, TX, United States

The increasing use of silver nanoparticles (nAg) in products and associated releases to the environment necessitates a thorough understanding of the environmental fate and transformations of these potentially toxic nanomaterials to inform environmental risk assessments. Herein, the physical and chemical transformations of nAg in natural lake water samples were investigated. Lake water systems containing filtered and unfiltered lake water (FLW and UFLW) were spiked with 80 nm polyvinylpyrrolidone-coated nAg (nAg_{pristine}) at 6 µg/L and were maintained under quiescent or mixed conditions in the dark for up to 44 days. Aliquots withdrawn from the water column contained smaller re-precipitated nAg (r-nAg, diameter ~26 nm) formed by precipitation of Ag⁺ released by oxidative dissolution of nAg_{pristine}. The number concentrations of r-nAg and nAg_{pristine} were comparable. In FLW, agglomerates of r-nAg and the partially dissolved nAg_{pristine} were formed under quiescent conditions and their settling accelerated after 14 days, but no settling occurred in the mixed systems. In UFLW, heteroagglomerates of r-nAg and the partially dissolved nAg_{pristine} with natural colloids formed and induced sedimentation in both quiescent and mixed systems. A fraction of the r-nAg formed and the larger (>40 nm) or primary n-Ag (comprised of partially dissolved nAg_{pristine} and its agglomerates with r-nAg or itself) were persistent in the water column for several weeks. Under quiescent conditions, more p-nAg remained suspended in FLW (15.7%, relative to number of nAg_{pristine} dosed) than in UFLW (5.9%), whereas more r-nAg persisted in UFLW (2.6%) than in FLW (0.6%). Thus, the size distributions and fractions of nAg persisting in the water column can change significantly depending on water chemistry and mixing conditions.

KEYWORDS

nanoparticle, fate and transport, Ag NPs, spICP, agglomeration

Introduction

Silver nanoparticles (nAg) are extensively used in consumer products due to their antimicrobial properties (Geranio et al., 2009; Mueller and Nowack, 2008; Parmar et al., 2022). The use of these products (e.g., cleaning and medical disinfection products, clothing) leads to the release of nAg to aquatic environments. In natural aquatic systems, nAg may undergo different physical/chemical transformation processes which influence their toxicity and bioavailability (Kaegi et al., 2011; Kittler et al., 2010; Kvitek et al., 2008; Levard et al., 2012; Levard et al., 2013; Park et al., 2011; Wu et al., 2023).

Physical transformations of nAg in natural waters include homoagglomeration (agglomeration between nAg) and heteroagglomeration (the attachment of nAg to natural colloids) (Wang et al., 2015). Agglomeration rates are influenced by the size, surface charge, the surface chemistry and the concentration of the natural colloids and nAg, and the chemistry (e.g., ionic strength, pH) of natural waters. Dissolved organic matter (DOM) can colloiddally stabilize nAg and natural colloids in aquatic systems through electrosteric forces (Fabrega et al., 2009; Sharma et al., 2014; Baalousha et al., 2013; Philippe and Schaumann, 2014) and lower agglomeration rates (Quik et al., 2014a; Song et al., 2023). In natural water systems, natural colloids may be present at concentrations tens of thousands of mg/L, orders of magnitude higher than $\mu\text{g/L}$ or ng/L level concentrations of nAg (or other engineered nanoparticles, ENPs), leading to more heteroagglomeration than homoagglomeration of nAg (Praetorius et al., 2014; Quik et al., 2014b).

Among chemical transformation process, oxidative dissolution of nAg under aerobic conditions in the presence and absence of UV light, has been widely studied (Azodi et al., 2016; Li et al., 2010; Liu and Hurt, 2010). The oxidative dissolution of nAg releases Ag^+ and reactive oxygen species, particularly superoxide ($\text{O}_2^{\cdot-}$) which leads to formation of hydrogen peroxide (Jones et al., 2011; Rong et al., 2018). The H_2O_2 formed can contribute to dissolution of nAg⁰ to Ag^+ (Rong et al., 2018). The superoxide also undergoes a series of reactions with nAg which involves electron transfers to form 'charged nAg' which reduces dissolved O_2 to $\text{O}_2^{\cdot-}$ and Ag^+ to nAg (He et al., 2012). The kinetics of the various reactions determine the net concentrations of Ag^+ and nAg at a given time. Re-precipitation of nAg from pristine nAg particles in wastewater effluents has been reported. The re-precipitation of nAg can be caused by sulfidation of Ag^+ dissolved from nAg, both by inorganic and organosulfur compounds, leading to formation of nAg₂S (Azodi et al., 2016; Ranjbari et al., 2022). Furthermore, studies have shown the reduction of Ag^+ to nAg can take place in the presence of DOM, (Adegboyega et al., 2013; Akaighe et al., 2011), particularly low molecular weight quinones (Wimmer et al., 2018). Exposure of Ag^+ to light can accelerate the reduction of Ag^+ to nAg by DOM (Hou et al., 2013; Yin et al., 2012), but is not essential for the precipitation reaction (Wimmer et al., 2018). Sulfidation of nAg in sulfidic natural waters can diminish dissolution rates due to the conversion of Ag^0 to insoluble Ag_2S (He et al., 2019).

Currently, no direct information is available on the abundance, size, and persistence of r-nAg in natural waters after their formation, and on their role in agglomeration processes. The majority of the studies assessing nAg transformation in aquatic systems have employed high initial Engineered Nanoparticles (ENP) concentrations owing to the limitations of the analytical techniques used for characterizing nAg concentrations, sizes, and speciation, with the exception of Wimmer et al. (2018). However, the use of high initial particle concentrations precludes the understanding of the nature and extent of dissolution, reformation and agglomeration behavior of nAg under environmentally relevant concentrations. Further, the studies generally focus on either physical or chemical transformations, and the interrelationships of the two have not been extensively studied (Li et al., 2010).

The objective of this study was to investigate the role of the physical and chemical transformation processes of dissolution, re-precipitation, and homo/hetero-agglomeration on the concentrations and size distributions of nAg particles (pristine and transformed), in model lake water systems. The model systems were maintained under quiescent and mixed conditions (representing turbulence in natural waters) and the water column was characterized for nAg sizes and concentration over time, up to 44 days. Both filtered and unfiltered lake water model systems were set up, to determine the effects of natural colloids on the physical and chemical transformation processes. Polyvinylpyrrolidone (PVP) coated nAg (PVP-nAg) of 80 nm diameter was added to the lake water model systems at 6 $\mu\text{g/L}$ (56 nM) to balance the emphasis on environmentally relevant concentrations. To investigate the behavior of nAg at environmentally relevant levels, a concentration of 6 $\mu\text{g/L}$ was selected. This concentration enabled reliable characterization of the size distributions and concentrations of nAg added, as well as any r-nAg formed (Zhang et al., 2019; Wimmer et al., 2019; Furtado et al., 2015). The size and concentration of nAg, as well dissolved Ag concentrations, were characterized primarily by single particle inductively coupled plasma mass spectrometry (spICP-MS), a sensitive analytical technique for the characterization of metal nanoparticles in complex aqueous matrices, and has been previously applied to monitor the size of nAg in experimental lake water systems (Rearick et al., 2018; Mitrano et al., 2014; Furtado et al., 2014).

Materials and methods

Lake water

Grab samples of lake water were collected approximately 1.5 m below the surface at Lac Hertel, at the Gault Nature Reserve (Mont-Saint-Hilaire, Quebec, Canada), McGill University, in pre-washed 2 L HDPE bottles and stored at 4°C until further use. Additional details of lake water analyses are presented in the Supplementary Information (Section 3, lake water analysis).

Lake water model systems

The lake water model systems were comprised of 120 mL graduated cylindrical glass bottles (inner diameter: 4.5 cm; height: 10 cm; headspace: 2 cm) and were wrapped in aluminum foil to prevent exposure to light. Parallel systems were employed containing unfiltered lake water (UFLW), filtered lake water (FLW, 0.1 μm). In the present study, PVP-coated silver nanoparticles were selected due to their superior colloidal stability in complex aqueous environments, and their widespread use in applications such as cosmetics, drug delivery, and water purification (Furtado et al., 2015; El-Shamy et al., 2023; Neto et al., 2023).

On day 0, PVP-coated nAg (PVP-coated NanoXact nAg⁰ (99.99% Ag purity, nanoComposix, nominal diameter of 80 nm) were added to yield a final concentration of 6 $\mu\text{g/L}$ (56 nM) and mixed for 60 s to disperse the particles in each lake water model system. Lake water model systems were maintained under quiescent conditions or were continuously mixed at 80 rpm on an orbital

shaker. The systems were aerobic throughout the experiment due to the presence of a headspace. Sample dilutions were performed immediately after sampling and the samples were analyzed promptly thereafter. The systems were sampled over a period of up to 45 days to determine changes in nAg size distributions and dissolved Ag concentrations. Aliquots (triplicates, 1 mL each) were periodically sampled 3 cm above the base carefully using a pipet (Schematic representation, [Supplementary Figure S1](#)). To examine the reproducibility of the experiment, triplicates of UFLW systems dosed with PVP-nAg and data obtained on day 7 is presented in the SI, [Supplementary Figure S14](#).

The final sampling time point for both quiescent and mixed UFLW systems corresponded to the time point when nAg concentrations were <10% of the initial spiked concentration, which is 44 days for the quiescent condition and 21 days for the mixed condition. FLW experiments were sampled until then to maintain uniformity.

As re-precipitation or reformation is a major fate process examined in this study, we established a control system to spike dissolved silver at various environmentally relevant concentrations. This approach aimed to better characterize the re-precipitation process under controlled conditions. To independently study the rate of formation of nAg from dissolved Ag, Ag⁺ was spiked (plasma CAL, 1000 mg/L, SCP Science, Canada) at 1, 10 and 1000 µg/L into UFLW and FLW. At 1 µg/L and 10 µg/L concentrations, the dilution factors are 10⁶ and 10⁵, respectively, from the 4% HNO₃ matrix contributed by the 1000 mg/L Ag standard. Due to the high dilution factor, the acid matrix is unlikely to impact the re-precipitation process in the control system. A similar methodology has been employed in our previous study, where the formation of nAg from dissolved Ag in wastewater effluents was reported ([Azodi et al., 2016](#)). All systems were set up in the dark under quiescent and mixed conditions in 50 mL polypropylene tubes (digiTubes, SCP Science, Canada). Control systems were set up in deionized (DI) water. All samples were analysed for nAg using spICP-MS.

Analytical techniques

PerkinElmer NexION 300X ICP-MS supported by Syngistix software (ver1.1.) was used in single particle mode for nAg characterization. The limits of detection for concentrations were established by measuring 80 nm PVP-nAg at different concentrations (5, 10, 20, 50 and 100 ng/L) in LW in triplicate under the specified instrument conditions (dwell time: 100 µs; analysis time: 100 s; using 57.1 nm nAu at a concentration of 170 ng/L to calculate transport efficiency). For 80 nm PVP-nAg, 10 ng/L corresponding to 11,464 ± 594 NP/mL was determined to be the limit of detection where reliable precision could be achieved. Additionally, the limit of detection for number concentration increased for particles smaller than 40 nm. For example, at 10 ng/L, 30 nm PVP-nAg exhibited a number concentration of 30,254 ± 1,015 NP/mL in LW. Further, the limit of detection for dissolved Ag concentration was 20 ng/L in lake water and 10 ng/L in deionized (DI) water and were determined by spiking dissolved silver and calculating recoveries from concentrations measured by the software. The dissolved silver measured by spICP-MS includes any free silver ions, soluble silver complexes, as well as small

nAg <15 nm, which are not detectable and are counted as dissolved silver. Other instrumental parameters ([Supplementary Table S1](#)) as well as total silver mass balances ([Supplementary Figure S2](#)) are reported as Supplementary Information.

Philips CM200 200 kV TEM with AMT XR40B CCD Camera and EDAX Genesis EDS analysis systems were used to image nAg and analyze elemental composition. Twenty µL of the concentrate was deposited on the Cu TEM substrates (Electron Microscopy Sciences, Carbon film 200 mesh Cu grids). The grids were kept in the dark and air-dried. The zeta potential and conductivity were determined using DLS (ZetaSizer Nano ZS, Malvern).

Statistical analysis

All experiments involving replicate measurements reported standard deviations to quantify variability. Where applicable, two-tailed t-tests were performed to compare means between groups, with significance determined at $p < 0.05$.

Results and discussion

Lake water characterization

The lake water had an electrical conductivity of 93.4 µS/cm and a pH of 7.5. Total suspended solids (TSS) in UFLW were 2.7 mg/L and negligible in FLW. It should be noted that natural colloids <100 nm may be present in both systems but could not be measured by TSS analysis. The natural colloid number concentration in the 35–1000 nm size range was determined to be $1.2 \pm 0.4 \times 10^8$ NP/mL ($n = 4$) with a mean diameter of 232.8 ± 57.8 nm using Nanoparticle Tracking Analysis (NTA NanoSight LM10, Malvern Panalytical). Because NTA cannot detect particles greater than 1000 nm ([Filipe et al., 2010](#)), the lake water was also characterized for colloids using laser diffraction (Horiba Laser Scattering Particle Size Analyzer). The average diameter detected by that technique was 7 µm (size distribution of 250 nm to 26 µm) ([Supplementary Figure S3](#)). The lake water was left undisturbed for ~6 months and the supernatant was analyzed using NTA to determine the non-settled fraction, which was determined to be $1.1 \pm 0.2 \times 10^8$ NP/mL ($n = 5$) ([Supplementary Figure S3](#)) with a mean diameter of 297 ± 24 nm. It should be noted that laser diffraction was not used to measure colloidal concentrations after 6 months, as larger particles were no longer expected to remain in suspension; therefore, only the non-settling fraction was analyzed using NTA. Dissolved organic carbon content (DOC) of UFLW and FLW was 3.5 ± 0.1 mg/L ($n = 3$) and 2.4 ± 0.1 mg/L ($n = 3$), respectively. nAg and dissolved Ag were not detected in unspiked UFLW and FLW by spICP-MS. Additional physicochemical and compositional characteristics of the lake water are shown in [Supplementary Table S2](#).

Characterization of silver nanoparticles

PVP-nAg added to the experimental systems had a mean diameter of 82 ± 14 nm ($n = 113$) as measured by TEM, and

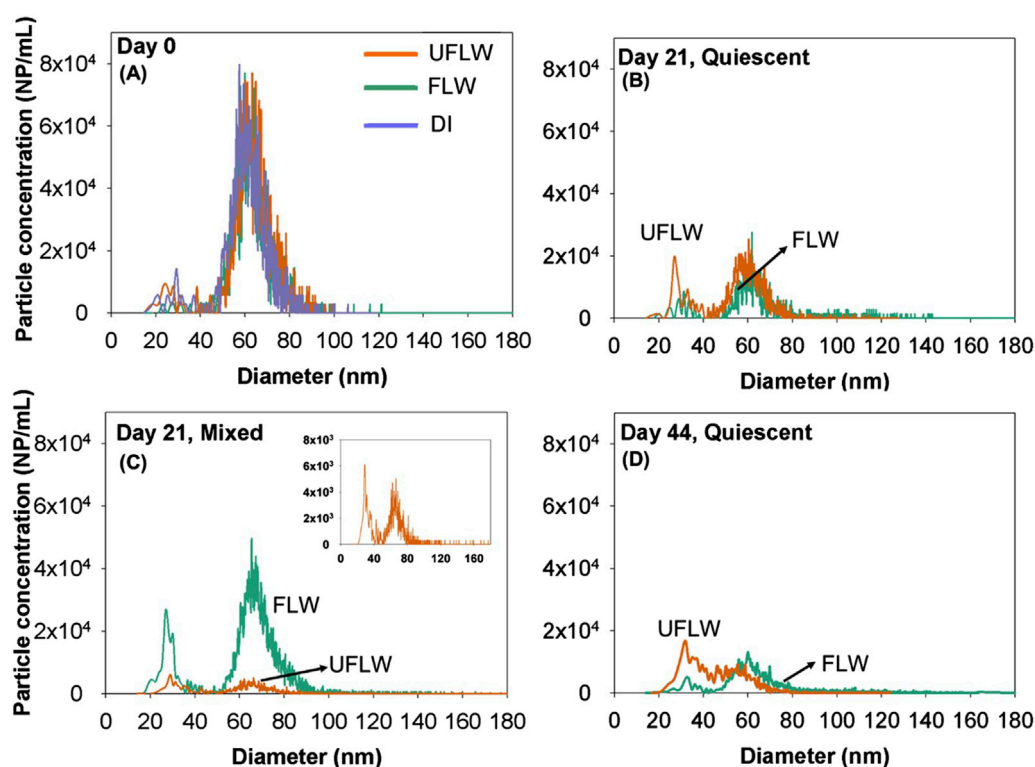


FIGURE 1 Particle size distribution of nAg on (A) Day 0 (B) quiescent conditions, Day 21 (C) mixed conditions, Day 21, Inset: Zoomed in particle size distribution of UFLW (D) Day 44 under quiescent conditions.

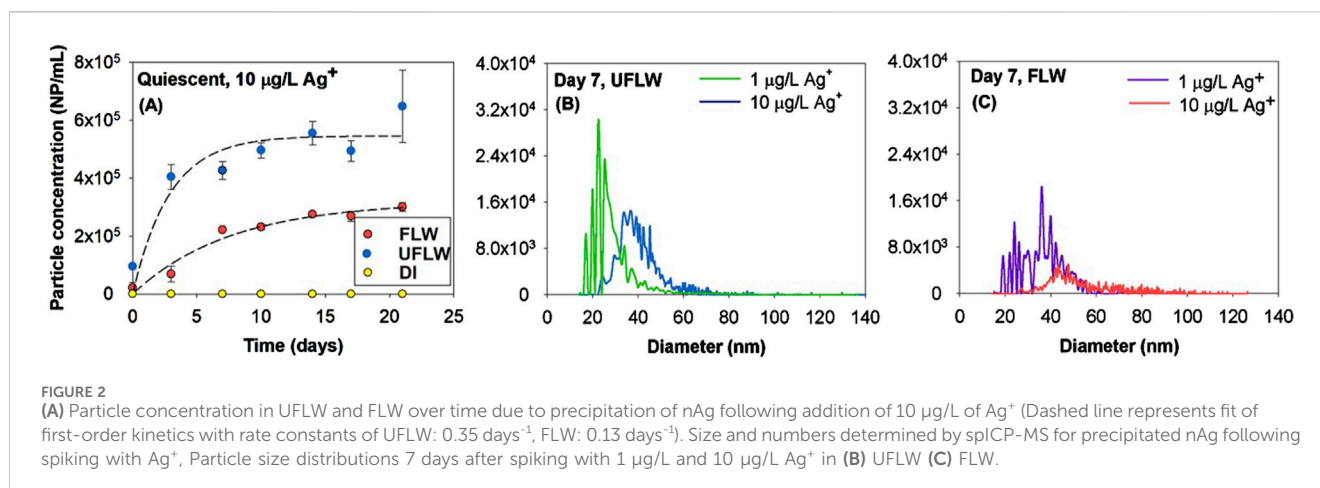
were primarily spherical (Supplementary Figure S4). spICP-MS analysis of the PVP-nAg in DI and UFLW yielded a mean diameter of 65.3 ± 6.9 nm and 64 ± 7 nm, respectively. The discrepancy between the TEM and spICP-MS measurements is attributable to the different particle population sizes measured, as spICP-MS did not account for the PVP coating, assuming perfect spherical particles. PVP-nAg was negatively charged in a 1.5 mM NaCl solution (-25.9 ± 2.8 mV).

Smaller nAg were formed after incubation of pristine nAg

FLW and UFLW systems were spiked with nAg_{pristine} and the nAg concentrations measured by spICP-MS immediately thereafter were 6.1 ± 0.3 $\mu\text{g/L}$ or $4 \times 10^6 \pm 1.8 \times 10^5$ NP/mL. Figure 1A shows the particle size distributions of nAg in DI, FLW and UFLW under quiescent conditions on day 0. The sizes were between 45 and 100 nm, and thus, this is designated as the primary nAg (p-nAg) population. All nAg particles measured in the >40 nm (pristine and homoagglomerated) range are hereafter referred to as p-nAg. It is important to note that we observed a few small signals corresponding to the <40 nm range in DI water, UFLW and FLW spiked with nAg, on day 0. These spikes are attributable to low concentrations of nAg that may have formed instantaneously (time scale of minutes) due to the reformation of Ag⁺ generated as observed by He et al. (2012). Alternatively, these small concentrations of <40 nm nAg could have been present in the stock PVP-nAg solutions.

An increase in number concentrations in <40 nm nAg range under mixed and quiescent conditions occurred on day 21 compared to day 0 (t-test, $p < 0.05$) in UFLW (Figure 1B) and FLW (Figure 1C) systems. For the DI water system under quiescent conditions (Supplementary Figure S5), there were no significant changes in particle size distributions between day 0 and day 21 (t-test, $p > 0.05$). However, an overall shift in particle size distribution towards smaller sizes was observed on day 44 (Figure 1D) compared to day 0 (mean diameter: day 0 = 63.5 ± 0.6 nm, day 21 = 59.7 ± 1.1 nm, day 44 = 57.3 ± 0.8 nm). No increase in <40 nm nAg was observed during the experimental period in the DI water system. As discussed later, sonication of all FLW and UFLW samples from day 21 and beyond indicated higher concentrations of r-nAg, confirming that r-nAg was present in significantly higher abundance. Sonication of day 0 samples did not enhance the particle concentrations (Supplementary Figure S6). The <40 nm nAg are referred to herein as re-precipitated (r-nAg) because they were formed by the DOM induced reduction/precipitation of dissolved Ag released by the primary nAg. A previous study attributed the low dissolved Ag from 11 nm citrate-nAg to re-precipitation in natural lake water (Ellis et al., 2018), however, the extent of re-precipitation was not quantified.

To verify if the r-nAg (<40 nm) particles in FLW and UFLW were derived from dissolution of nAg_{pristine}, the lake water samples were spiked with Ag⁺ (1 and 10 $\mu\text{g/L}$) and incubated in the absence of light under quiescent and mixed conditions. In control systems, Ag⁺ was spiked in DI water, which did not result in formation of nAg at any time under those incubation conditions. Formation of nAg



was immediately observed (Supplementary Figure S6) in UFLW systems (9.4×10^4 NP/mL or 4.7 ng/L at 1 h) but formation of nAg in FLW was slower (Figure 2A). FLW had lower DOC (2.37 mg/L) than UFLW (3.48 mg/L), which likely contributed to the slower formation and fewer nAg. Similar effects of DOC concentrations on nAg formation have been reported elsewhere (Wimmer et al., 2018).

Figures 2B, C represent particle size distributions of nAg formed in UFLW and FLW under quiescent conditions 7 days after being spiked with 1 µg/L and 10 µg/L of Ag⁺. The estimated mean diameters of nAg in UFLW (Figure 2B) on day 7 using spICP-MS were determined to be 28.8 ± 3.9 nm and 44.3 ± 8.1 nm at spiked Ag⁺ concentrations of 1 µg/L and 10 µg/L, respectively. In FLW systems (Figure 2C), estimated mean diameters were slightly higher compared to UFLW systems, with 36.3 ± 3.8 nm at 1 µg/L Ag⁺ and 60.3 ± 12.6 nm at 10 µg/L Ag⁺ on day 7. There was no further increase in mean diameters over the incubation period of 30 days (Supplementary Figure S7). Higher concentration of Ag⁺ (1000 µg/L) was spiked for TEM analysis (Supplementary Figure S7) where, diameters of precipitated nAg in UFLW was 49 ± 17.9 (n = 93) and 61.3 ± 16.8 nm (n = 71) in FLW. TEM images (Supplementary Figure S7) reveal precipitated nAg associated with organic matter which is confirmed with the high carbon signal observed in the EDS analysis of the precipitated nAg. The particle images observed in this study are similar to those in a recent study of asymmetric silver nanoparticle structures formed by spiking Ag⁺ into a synthetic polymer solution (Li et al., 2019). A high-contrast silver nanoparticle was associated with a lower-contrast region, which comprised of low amounts of silver and polymer. Formation of nAg of similar diameter and concentrations in FLW and UFLW as above was also observed under mixed conditions (Supplementary Figure S8).

In the lake water model systems, the maximum dissolved Ag was 0.22 and 0.07 µg/L in FLW and UFLW, respectively, under mixed conditions and 0.28 µg/L in FLW and 0.16 µg/L in UFLW under quiescent conditions (Supplementary Figure S9). Thus the size of r-nAg was close to nAg formed with 1 µg/L Ag⁺. Previous studies on precipitation of nAg by DOM of Ag⁺ were conducted with Ag⁺ concentrations in the mg/L range (Hou et al., 2013; Yin et al., 2012). To date, only one study has demonstrated DOM-reduced formation of nAg with comparable Ag⁺ concentrations (50 ng/L) (Wimmer et al., 2018).

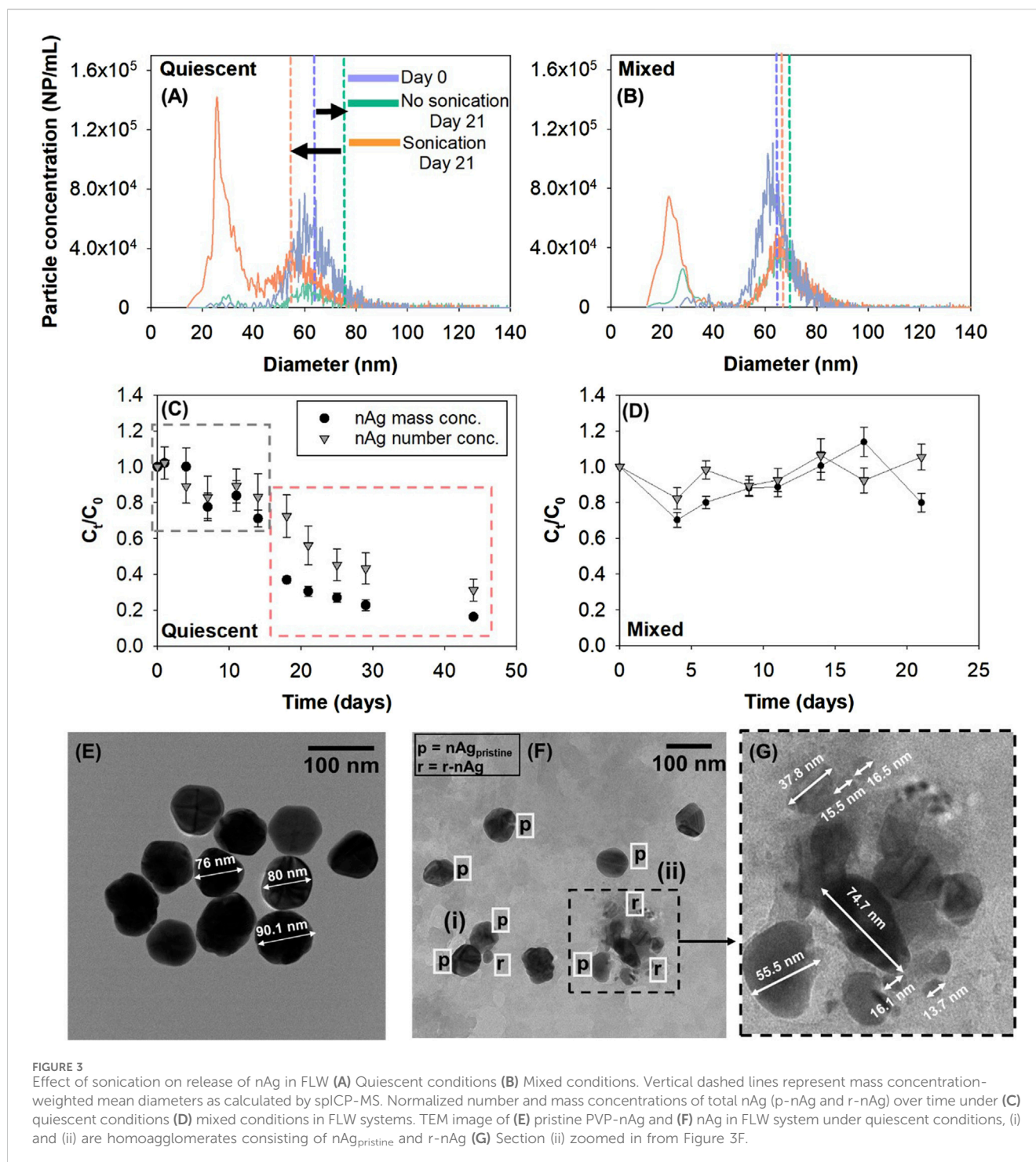
In FLW, homoagglomeration determines the sizes and concentrations of p-nAg and r-nAg

In the absence of colloids (FLW) and under quiescent conditions, a shift to larger sizes with a statistically significant ~ 10 nm increase in particle diameters (paired t-test, $p < 0.05$) was observed after 21 days compared to day 0 (Figure 3A), suggesting homoagglomeration. To determine the extent of homoagglomeration of nAg in FLW, samples taken at different time points from the test vials were immediately sonicated for 5 min (37 kHz, Fisherbrand ultrasonic water bath) to thoroughly disagglomerate (Huynh and Chen, 2014) and disperse r-nAg and nAg_{pristine}. Sonication yielded (i) smaller sizes of p-nAg, with the most frequent size measured decreased from 61.4 ± 0.3 nm to 25.3 ± 0.4 nm and (ii) a 29-fold increase (release of 1.07×10^6 NP/mL) in r-nAg number concentration upon sonication (Figure 3A). Sonication also caused a 2.5-fold increase in number concentration of p-nAg, as a consequence of the break up of larger homoagglomerates (80–140 nm). An increase in measured sizes due to agglomeration of citrate-nAg was also observed elsewhere in a filtered lake water sample (Ellis et al., 2018).

In mixed systems (Figure 3B), sonication yielded 2.7×10^5 NP/mL of r-nAg after 21 days, which was 2.5 times higher than non-sonicated samples and approximately 6-times lower than r-nAg released from sonication of samples from the quiescent systems.

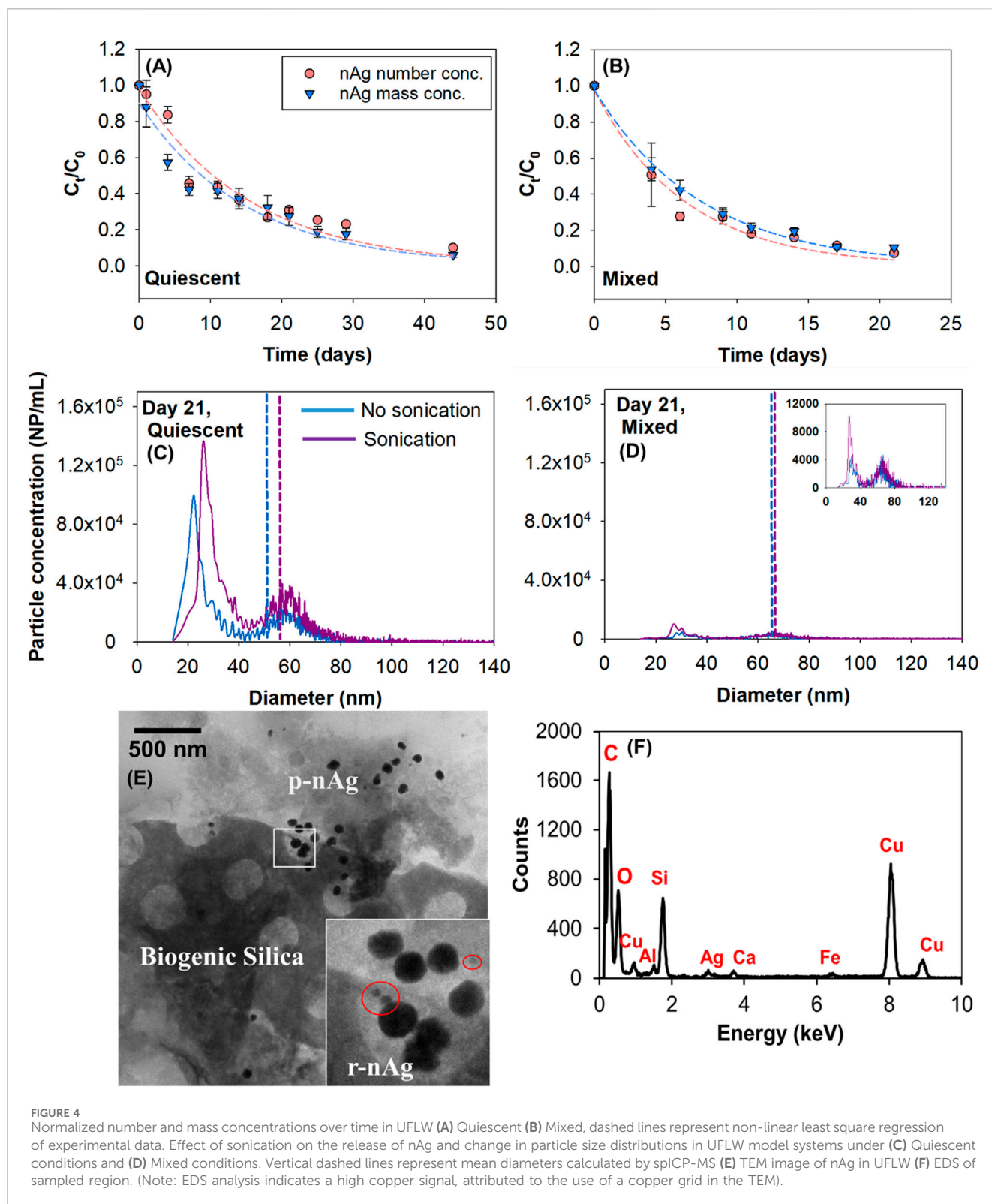
There was no significant change in nAg >40 nm particle concentrations in line with the lower extent of agglomeration in mixed systems. Higher dissolved Ag concentrations (0.22 µg/L) were measured in mixed systems on day 21 compared to quiescent systems where measured dissolved Ag concentrations were negligible (Supplementary Figure S8). This suggests that mixing resulted in unfavourable conditions for r-nAg formation from dissolved Ag.

In order to quantify homoagglomeration, particle number and mass concentrations in the suspension were evaluated over time. In quiescent systems (Figure 3C), there was relatively limited change in particle mass and number concentrations over the first 14 days (C_t/C_0 , number conc. decreased to 0.71) than in the subsequent 14-day period (C_t/C_0 , number conc. = 0.23), suggesting an initial phase of low agglomeration and sedimentation rate, followed by an increase in both of these processes. These patterns are clearly reflected in the



analyses of particle size distribution of non-sonicated samples of day 0, 14 and 18. (Supplementary Figure S9). Based on these results, the nAg concentration time profiles can be classified into two regimes: (i) decrease in nAg concentrations independent of homoagglomeration (black dashed box) (ii) homoagglomeration-induced sedimentation (red dashed box). In the absence of homoagglomeration and sedimentation, the number and mass concentration should remain unchanged over time. In the presence of homoagglomeration, the number concentration of NPs at a given time point would decrease while yielding the

same mass concentration. Decreases in particle mass concentration is attributable solely to sedimentation. The change in mass concentration in the homoagglomeration regime was used to calculate a rate constant for sedimentation ($k_{\text{homo, sed}}$) of 0.036 days^{-1} (Supplementary Figure S10). In contrast, with the systems where Ag^+ was added to the FLW and maintained under quiescent conditions there was no reduction in particle concentrations over time, suggesting that sedimentation occurs only in the nAg spiked FLW systems. In other studies, nAg formed in the presence of DOM (and indoor light) after the



addition of Ag^+ was found to be stable for up to 180 days, although the DOM concentrations were much higher than in this study (Hou et al., 2013; Yin et al., 2012).

In mixed systems, total particle number concentrations ($3.5 \pm 0.7 \times 10^6$ NP/mL) remained effectively unchanged over the experimental period of 21 days (Figure 3D). The mixing energy

was likely sufficient to keep the r-nAg and p-nAg suspended, and may have increased interactions of nAg_{pristine} and/or r-nAg with DOM leading to their higher steric stabilization, and limited homoagglomeration (Keller et al., 2010).

Figures 3E–G show TEM images of pristine nAg and nAg agglomerates formed in FLW. The agglomerate cluster in

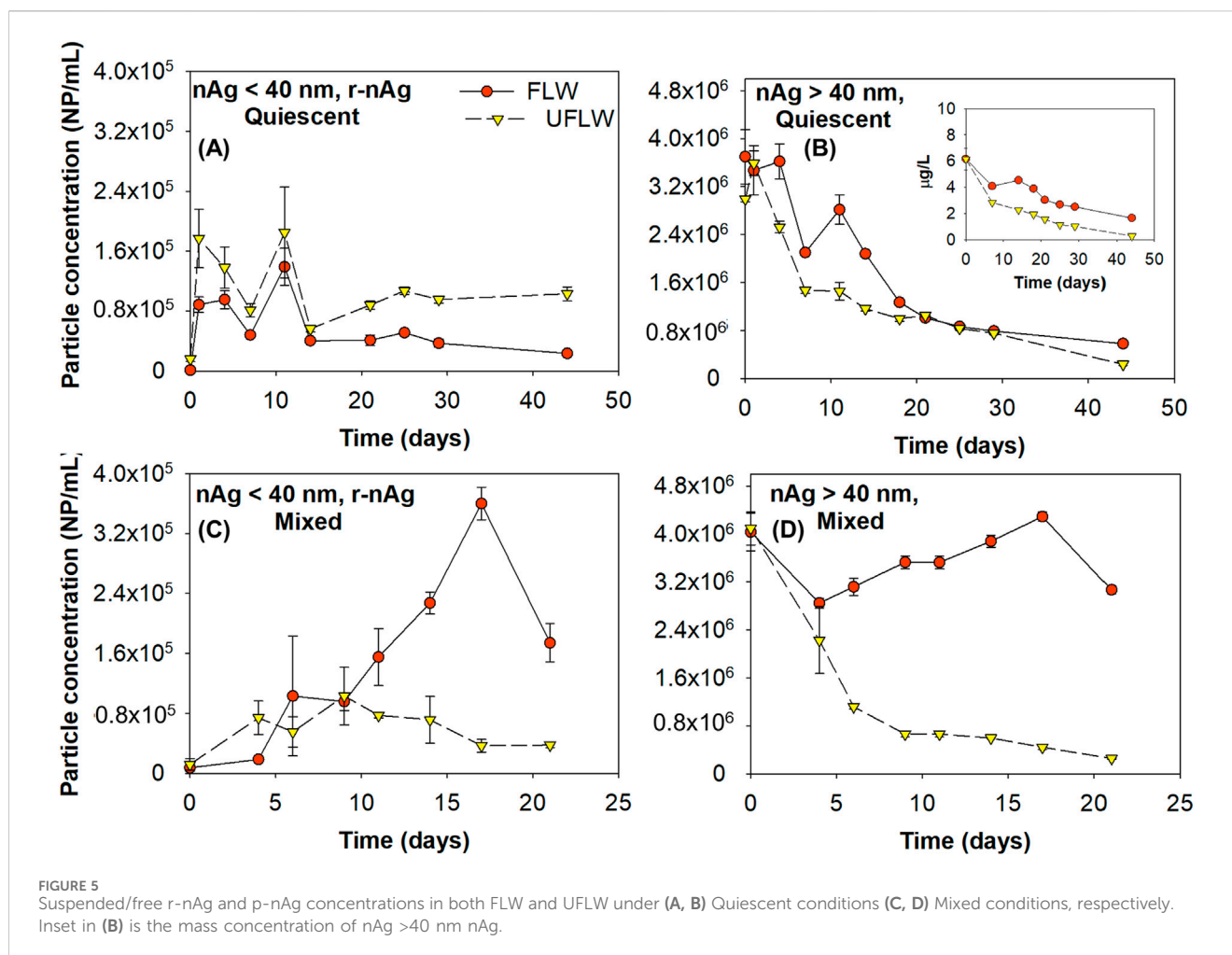


Figure 3F has (i) two p-nAg (~70 nm) and one r-nAg (28 nm) and (ii) has 7 r-nAg and p-nAg particles ranging from 6 nm to 75 nm in diameter. Overall, the data suggests for nAg in FLW under quiescent conditions, homoagglomeration between p-nAg/r-nAg, r-nAg/r-nAg and p-nAg/p-nAg occurred, and led to sedimentation.

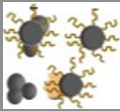
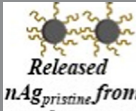
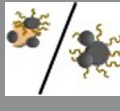
In unfiltered lake water natural colloids influence the concentration of primary and re-precipitated nAg in the water column

In the presence of colloids, the fate of nAg was more complex with potentially more heterogeneous interactions (p-nAg, r-nAg and natural colloids) occurring in system. A decrease in total nAg particle number and mass concentrations over time was observed in quiescent and mixed systems in the presence of colloids (Figures 4A, B), with a faster decrease in mixed systems. After 21 days under mixed conditions, only 3.1×10^5 NP/mL (7% of initial spiked particle number concentration) were detected in quiescent systems. This is different from the FLW mixed systems where there was no effective decrease in nAg concentrations. Sedimentation rate constants were estimated to be 0.06 days^{-1} and 0.13 days^{-1} under quiescent and mixed conditions, respectively and were obtained by fitting the mass concentration over time in Figures 4A, B (Supplementary Figure S11).

A 2.2-fold increase in sedimentation rate constant in the mixed system compared to the quiescent system can be attributed to increased collisions between nAg and natural colloids (heteroagglomeration) owing to the external mixing (Walters et al., 2013; Ilona and Dik, 2014). These sedimentation results are consistent with the results obtained by Velzeboer et al., who showed that sedimentation rate constants were between one and two orders of magnitude higher in mixed systems compared to stagnant systems (Velzeboer et al., 2014).

Due to the complexity of the system, it is challenging to differentiate the impacts of sedimentation and agglomeration occurring in UFLW. Nevertheless, as explained in the previous section; if there is homoagglomeration, the following phenomena should occur; (a) shift in particle size distribution upon sonication (b) C_t/C_0 trends of number and mass concentrations should differ due to lower number concentrations compared to mass concentrations. Unlike the trends observed in FLW systems (Figure 3A), there is no significant difference between mass and number normalized concentrations over time (Figures 4A, B) in UFLW systems (paired t-test, $p > 0.05$). The number concentration of natural colloids was determined to be approximately 200 times greater than the spiked PVP-nAg suggesting heteroagglomeration between PVP-nAg and the natural colloids as the dominant process influencing nAg concentrations. TEM images of UFLW sampled

TABLE 1 Summary of the distribution of r-nAg and p-nAg in Mont St. Hilaire lake water in the presence and absence of colloids on day 21 and day 44, respectively. The values reported in percentages are concentrations of nAg or dissolved Ag present relative to the initial dosed nAg_{pristine} concentration.

System	Suspended nAg 40 nm	After Sonication		Suspended nAg < 40 nm (r-nAg)	Dissolved Ag	Settled fraction, All nAg sizes
	 (1)	 (1A)	 (1B)	 (2)	 (3)	 (4) = Initial - (1) - (2) - (3)
Mass concentration						
FLW _{mixed} , 21d	105.0%	0.02 µg/L	-	0.4%	3.5%	-
UFLW _{mixed} , 21d	9.8%	0.004 µg/L	0.2 µg/L	0.1%	1.1%	89.4%
FLW _{quiescent} , 21d	0.1%	0.15 µg/L	1.9 µg/L	54.9%	0.0%	52.7%
UFLW _{quiescent} , 21d	0.3%	0.06 µg/L	2.2 µg/L	25.1%	2.5%	73.0%
FLW _{quiescent} , 44d	28.9%	0.05 µg/L	-	0.1%	2.8%	67.0%
UFLW _{quiescent} , 44d	4.5%	-	0.3 µg/L	0.3%	4.6%	89.6%
Number concentration						
FLW _{mixed} , 21d	75.3%	2.7 × 10 ⁵ NP/mL	-	4.3%	-	20.5%
UFLW _{mixed} , 21d	6.4%	2.5 × 10 ⁴ NP/mL	6 × 10 ⁴ NP/mL	0.9%	-	92.7%
FLW _{quiescent} , 21d	27.3%	1.1 × 10 ⁶ NP/mL	1.5 × 10 ⁶ NP/mL	1.1%	-	69.5%
UFLW _{quiescent} , 21d	28.4%	1.6 × 10 ⁵ NP/mL	1.1 × 10 ⁶ NP/mL	2.5%	-	69.0%
FLW _{quiescent} , 44d	15.7%	5.6 × 10 ⁵ NP/mL	1.8 × 10 ⁶ NP/mL	0.6%	-	83.8%
UFLW _{quiescent} , 44d	5.9%	-	4.2 × 10 ⁴ NP/mL	2.6%	-	89.9%

near the bottom on the lake water model system revealed presence of nAg with structures that resemble biogenic silica (Mann, 1986). EDS confirmed the presence of Ag⁰ and Si (Figures 4E, F). In FLW, no such natural colloid elements were detected using EDS (Supplementary Figure S12).

Sonication led to small increases in r-nAg number concentrations in UFLW samples (Figures 4C, D). Under quiescent conditions, a release of 1.1 × 10⁶ NP/mL upon sonication (15.4% was <40 nm and 84.6% was >40 nm) after 21 days was observed. A release of 7.5 × 10⁴ NP/mL (33.4% was <40 nm and 66.6% was >40 nm) was observed under mixed conditions. However, the absence of any significant shift in particle size distributions upon sonication in the presence of colloids (mixed and quiescent), along with the similar rates of change in particle and number and mass concentrations suggest that heteroagglomeration-induced sedimentation was the predominant phenomena in UFLW systems.

Silver nanoparticles are persistent in suspension over several weeks

A measureable fraction of p-nAg and r-nAg were present in suspension at the end of 21 days or 44 days in all systems (Figures 5A–D). In Table 1, Column 1 shows the mass and number fractions

remaining in the water column and was quantified based on analysis of the non-sonicated samples (includes nAg_{pristine} and agglomerates of p-nAg and r-nAg). The difference in sonicated and non-sonicated samples was calculated to determine the fraction of r-nAg (Table 1, Column 1A) and nAg_{pristine} (Table 1, Column 1B) that was agglomerated. The settled fraction (Table 1, Column 4) was estimated as the difference between the initial spiked concentration and the suspended and dissolved concentrations.

Table 1 shows that for p-nAg, in both the quiescent condition and the mixed condition, at the end of the incubation period (21 days for mixed systems and 44 days for the quiescent systems), more particles remained in suspension in the FLW system (75.3% for mixed system and 15.7% for quiescent system) compared to the UFLW system (6.4% for the mixed system and 5.9% for the quiescent system). This can be attributed to more sedimentation induced by heteroagglomeration between nAg and natural colloids in UFLW. Similar trends were observed for r-nAg under mixed conditions with higher amounts of r-nAg present in the FLW (4.3%) compared to UFLW (0.9%). Both heteroagglomeration, and the lower amounts of r-nAg formed in UFLW (Figures 3B, 4D) are underlying causes. However, under quiescent conditions, more r-nAg remained in the suspension in UFLW (2.6%) compared to FLW (0.6%), even though

comparable numbers of r-nAg were formed in the two systems (Figures 3A, 4C).

The extended presence of both p-nAg and r-nAg in the water column in UFLW systems is likely because (i) heteroagglomeration between nAg and natural colloids was much slower than the sedimentation of the natural colloids, making heteroagglomeration the rate-limiting step, and (ii) the natural colloids in suspension at the end of the experiment were colloidally stable with negligible settling velocity. Even after 6-month of quiescent incubation the natural colloid concentrations were ~10% of the initial number count, as obtained using NTA (35–400 nm diameter), confirming the presence of a stable fraction of natural colloids.

Persistence of nAg in the water column has also been reported elsewhere with 3.8% of 500 µg/L PVP-nAg suspension in river water remaining at the end of 14 days under mixed conditions (Velzeboer et al., 2014). In the absence of mixing, 23.2% of the spiked 500 µg/L PVP-nAg was still in suspension in fresh water at the end of 14 days (Quik et al., 2014a). In another study, PVP-nAg (~11 nm, dosed at 100 µg/L) in a lake water model system was reported to be persistent in the water column for up to 28 days (Ellis et al., 2018). In a whole-lake experiment research where PVP-coated nAg was spiked into an experimental lake, ~28% colloidal Ag was also identified to remain in suspension (Furtado et al., 2015). Although persistence of nAg in the water column was investigated before, no characterization on the speciation and particle number concentration of nAg was performed. Furthermore, those previous studies have evaluated colloidal stability of nAg in natural waters by dosed at concentrations at least 10-times higher than this study. By using sp-ICP-MS, this study demonstrated that a fraction of both nAg_{pristine} and r-nAg remain colloidally stable, while the remained settles after homo and heteroagglomeration, even when nAg_{pristine} is added at a low, close to environmentally relevant concentration for surface waters of 6 µg/L. This study also highlights the importance of investigating both the particle mass and particle number concentrations when investigating the behavior of NPs in the water system. Under mixed conditions, the r-nAg mass concentration remaining in the FLW and UFLW water column was only 0.4% and 0.1%, respectively, of the initial nAg_{pristine} mass concentration. However, this represents 4.3% and 0.9% of the initial particle concentration. Particle sizes and concentrations provide data on particle surface areas, which may provide an alternative basis for toxicity and risk potential. Only reporting mass concentration of NPs in the water system might thus resulted in biased understanding of their potential risks.

Conclusion

Ag⁺ released by dissolution from 80 nm PVP-coated nAg_{pristine} was precipitated as r-nAg⁰ with a mean diameter of 25.6 ± 0.7 nm, thus dramatically changing the particle size distributions over time. The reaction occurred under dark conditions in both FLW and UFLW and mixed and quiescent systems. Fewer r-nAg were formed in mixed systems compared to quiescent systems for both FLW and UFLW. Homoagglomeration of r-nAg and nAg_{pristine} was the

dominant fate process in the absence of natural colloids (FLW), whereas heteroagglomeration of both r-nAg and p-nAg with natural colloids dominated in UFLW. The sedimentation rates of total nAg mass was higher in UFLW than in FLW, and heteroaggregation was a more dominant process for removal of nAg from the aqueous phase. At the end of the experiments (21 days for mixed systems and 44 days for quiescent systems), varying amounts of r-nAg and p-nAg remained in the water column depending on the system conditions.

Current ENP fate and transport models and risk assessments do not account for formation of re-precipitated particles and their fate in aquatic ecosystems. The detailed size distribution data from sp ICP-MS analysis presented herein will be used to support modeling of the re-precipitation and their agglomeration behavior in future studies, towards providing a more robust analysis of Ag fate in aquatic systems. Detailed characterization of nAg speciation using sensitive techniques, as reported in this study, is important for thorough quantitative assessments of fate processes, and characterization based on mean diameters and total Ag concentrations.

Data availability statement

The raw data supporting the conclusions of this article will be made available by the authors, without undue reservation.

Author contributions

SR: Data curation, Formal Analysis, Investigation, Methodology, Validation, Visualization, Writing–original draft. XG: Formal Analysis, Investigation, Writing–review and editing. SG: Conceptualization, Data curation, Formal Analysis, Funding acquisition, Investigation, Methodology, Project administration, Supervision, Validation, Writing–review and editing.

Funding

The author(s) declare that financial support was received for the research, authorship, and/or publication of this article. The research was supported by the Natural Sciences and Engineering Research Council of Canada (Grant nos. STPGP 430659–12, RGPIN-2016-05022, RGPAS 492998), Environment and Climate Change Canada, Fonds de recherche du Québec-Secteur Nature et Technologies - Strategic Clusters (RS-265155), and Cascades Canada ULC. SR was supported by a McGill Engineering Doctoral Award.

Acknowledgments

We acknowledge the assistance of David Liu, McGill University, for TEM/EDS analysis. Dr. Yanyan Zhang provided comments to improve the manuscript and figures.

Conflict of interest

The authors declare that the research was conducted in the absence of any commercial or financial relationships that could be construed as a potential conflict of interest.

The author(s) declared that they were an editorial board member of Frontiers, at the time of submission. This had no impact on the peer review process and the final decision.

Generative AI statement

The author(s) declare that no Generative AI was used in the creation of this manuscript.

References

- Adegboyega, N. F., Sharma, V. K., Siskova, K., Zbořil, R., Sohn, M., Schultz, B. J., et al. (2013). Interactions of aqueous Ag⁺ with fulvic acids: mechanisms of silver nanoparticle formation and investigation of stability. *Environ. Sci. and Technol.* 47 (2), 757–764. doi:10.1021/es302305f
- Akaighe, N., MacCuspie, R. I., Navarro, D. A., Aga, D. S., Banerjee, S., Sohn, M., et al. (2011). Humic acid-induced silver nanoparticle formation under environmentally relevant conditions. *Environ. Sci. and Technol.* 45 (9), 3895–3901. doi:10.1021/es103946g
- Azodi, M., Sultan, Y., and Ghoshal, S. (2016). Dissolution behavior of silver nanoparticles and formation of secondary silver nanoparticles in municipal wastewater by single-particle ICP-MS. *Environ. Sci. and Technol.* 50 (24), 13318–13327. doi:10.1021/acs.est.6b03957
- Baalousha, M., Nur, Y., Römer, I., Tejamaya, M., and Lead, J. R. (2013). Effect of monovalent and divalent cations, anions and fulvic acid on aggregation of citrate-coated silver nanoparticles. *Sci. Total Environ.* 454–455, 119–131. doi:10.1016/j.scitotenv.2013.02.093
- Ellis, L.-J. A., Baalousha, M., Valsami-Jones, E., and Lead, J. R. (2018). Seasonal variability of natural water chemistry affects the fate and behaviour of silver nanoparticles. *Chemosphere* 191, 616–625. doi:10.1016/j.chemosphere.2017.10.006
- El-Shamy, O. A., El-Adawy, M. M., and Abdelsalam, M. (2023). Chemical synthesis of a polyvinylpyrrolidone-capped silver nanoparticle and its antimicrobial activity against two multidrug-Resistant *Aeromonas* species. *Aquac. Res.* 2023 (1), 1–9. doi:10.1155/2023/3641173
- Fabrega, J., Renshaw, J. C., and Lead, J. R. (2009). Interactions of silver nanoparticles with *Pseudomonas putida* biofilms. *Environ. Sci. and Technol.* 43 (23), 9004–9009. doi:10.1021/es901706j
- Filipe, V., Hawe, A., and Jiskoot, W. (2010). Critical evaluation of Nanoparticle Tracking Analysis (NTA) by NanoSight for the measurement of nanoparticles and protein aggregates. *Pharm. Res.* 27 (5), 796–810. doi:10.1007/s11095-010-0073-2
- Furtado, L. M., Hoque, M. E., Mitrano, D. M., Ranville, J. F., Cheever, B., Frost, P. C., et al. (2014). The persistence and transformation of silver nanoparticles in littoral lake mesocosms monitored using various analytical techniques. *Environ. Chem.* 11 (4), 419–430. doi:10.1071/en14064
- Furtado, L. M., Norman, B. C., Xenopoulos, M. A., Frost, P. C., Metcalfe, C. D., and Hintelmann, H. (2015). Environmental fate of silver nanoparticles in boreal lake ecosystems. *Environ. Sci. and Technol.* 49 (14), 8441–8450. doi:10.1021/acs.est.5b01116
- Geranio, L., Heuberger, M., and Nowack, B. (2009). The behavior of silver nanotextiles during washing. *Environ. Sci. and Technol.* 43 (21), 8113–8118. doi:10.1021/es901833z
- He, D., Garg, S., and Waite, T. D. (2012). H₂O₂-Mediated oxidation of zero-valent silver and resultant interactions among silver nanoparticles, silver ions, and reactive oxygen species. *Langmuir* 28 (27), 10266–10275. doi:10.1021/la300929g
- He, D., Garg, S., Wang, Z., Li, L., Rong, H., Ma, X., et al. (2019). Silver sulfide nanoparticles in aqueous environments: formation, transformation and toxicity. *Environ. Sci. Nano* 6, 1674–1687. doi:10.1039/c9en00138g
- Hou, W.-C., Stuart, B., Howes, R., and Zepp, R. G. (2013). Sunlight-driven reduction of silver ions by natural organic matter: formation and transformation of silver nanoparticles. *Environ. Sci. and Technol.* 47 (14), 7713–7721. doi:10.1021/es400802w
- Huynh, K. A., and Chen, K. L. (2014). Disaggregation of heteroaggregates composed of multiwalled carbon nanotubes and hematite nanoparticles. *Environ. Sci. Process. and Impacts* 16 (6), 1371–1378. doi:10.1039/c3em00688c
- Ilona, V. T. K. Q. J., and Dik, vdM. A. K. A. (2014). Rapid settling of nanoparticles due to heteroaggregation with suspended sediment. *Environ. Toxicol. Chem.* 33 (8), 1766–1773. doi:10.1002/etc.2611
- Jones, A. M., Garg, S., He, D., Pham, A. N., and Waite, T. D. (2011). Superoxide-mediated formation and charging of silver nanoparticles. *Environ. Sci. and Technol.* 45 (4), 1428–1434. doi:10.1021/es103757c
- Kaegi, R., Voegelin, A., Sinnert, B., Zuleeg, S., Hagendorfer, H., Burkhardt, M., et al. (2011). Behavior of metallic silver nanoparticles in a pilot wastewater treatment plant. *Environ. Sci. and Technol.* 45 (9), 3902–3908. doi:10.1021/es1041892
- Keller, A. A., Wang, H., Zhou, D., Lenihan, H. S., Cherr, G., Cardinale, B. J., et al. (2010). Stability and aggregation of metal oxide nanoparticles in natural aqueous matrices. *Environ. Sci. and Technol.* 44 (6), 1962–1967. doi:10.1021/es902987d
- Kittler, S., Greulich, C., Diendorf, J., Köller, M., and Eppler, M. (2010). Toxicity of silver nanoparticles increases during storage because of slow dissolution under release of silver ions. *Chem. Mater.* 22 (16), 4548–4554. doi:10.1021/cm100023p
- Kvítek, L., Panáček, A., Soukupová, J., Kolář, M., Večeřová, R., Prucek, R., et al. (2008). Effect of surfactants and polymers on stability and antibacterial activity of silver nanoparticles (NPs). *J. Phys. Chem. C* 112 (15), 5825–5834. doi:10.1021/jp711616v
- Levard, C., Hotze, E. M., Lowry, G. V., and Brown, G. E. (2012). Environmental transformations of silver nanoparticles: impact on stability and toxicity. *Environ. Sci. and Technol.* 46 (13), 6900–6914. doi:10.1021/es2037405
- Levard, C., Mitra, S., Yang, T., Jew, A. D., Badireddy, A. R., Lowry, G. V., et al. (2013). Effect of chloride on the dissolution rate of silver nanoparticles and toxicity to *E. coli*. *Environ. Sci. and Technol.* 47 (11), 5738–5745. doi:10.1021/es400396f
- Li, R., Wang, H., Song, Y., Lin, Y.-N., Dong, M., Shen, Y., et al. (2019). *In situ* production of Ag/polymer asymmetric nanoparticles via a powerful light-driven technique. *J. Am. Chem. Soc.* 141, 19542–19545. doi:10.1021/jacs.9b10205
- Li, X., Lenhart, J. J., and Walker, H. W. (2010). Dissolution-accompanied aggregation kinetics of silver nanoparticles. *Langmuir* 26 (22), 16690–16698. doi:10.1021/la101768n
- Liu, J., and Hurt, R. H. (2010). Ion release kinetics and particle persistence in aqueous nano-silver colloids. *Environ. Sci. and Technol.* 44 (6), 2169–2175. doi:10.1021/es9035557
- Mann, S., and Perry, C. C. (1986). Structural aspects of biogenic silica. *Silicon Biochem.*, 40. doi:10.1002/9780470513323.ch4
- Mitrano, D., Ranville, J. F., Bednar, A., Kazor, K., Hering, A. S., and Higgins, C. P. (2014). Tracking dissolution of silver nanoparticles at environmentally relevant concentrations in laboratory, natural, and processed waters using single particle ICP-MS (spICP-MS). *Environ. Sci. Nano* 1 (3), 248–259. doi:10.1039/c3en00108c
- Mueller, N. C., and Nowack, B. (2008). Exposure modeling of engineered nanoparticles in the environment. *Environ. Sci. and Technol.* 42 (12), 4447–4453. doi:10.1021/es7029637
- Neto, F. N. S., Morais, L. A., Gorup, L. F., Ribeiro, L. S., Martins, T. J., Hosida, T. Y., et al. (2023). Facile synthesis of PVP-Coated silver nanoparticles and evaluation of their physicochemical, antimicrobial and toxic activity. *Colloids Interfaces* 7 (4), 66. doi:10.3390/colloids7040066
- Park, MVDZ, Neigh, A. M., Vermeulen, J. P., de la Fonteyne, L. J. J., Verharen, H. W., Briedé, J. J., et al. (2011). The effect of particle size on the cytotoxicity, inflammation, developmental toxicity and genotoxicity of silver nanoparticles. *Biomaterials* 32 (36), 9810–9817. doi:10.1016/j.biomaterials.2011.08.085

Publisher's note

All claims expressed in this article are solely those of the authors and do not necessarily represent those of their affiliated organizations, or those of the publisher, the editors and the reviewers. Any product that may be evaluated in this article, or claim that may be made by its manufacturer, is not guaranteed or endorsed by the publisher.

Supplementary material

The Supplementary Material for this article can be found online at: <https://www.frontiersin.org/articles/10.3389/fenvc.2025.1511440/full#supplementary-material>

- Parmar, S., Kaur, H., Singh, J., Matharu, A. S., Ramakrishna, S., and Bechelany, M. (2022). Recent advances in green synthesis of Ag NPs for extenuating antimicrobial resistance. *Nanomaterials* 12 (7), 1115. doi:10.3390/nano12071115
- Philippe, A., and Schaumann, G. E. (2014). Interactions of dissolved organic matter with natural and engineered inorganic colloids: a review. *Environ. Sci. and Technol.* 48 (16), 8946–8962. doi:10.1021/es502342r
- Praetorius, A., Labille, J., Scheringer, M., Thill, A., Hungerbühler, K., and Bottero, J.-Y. (2014). Heteroaggregation of titanium dioxide nanoparticles with model natural colloids under environmentally relevant conditions. *Environ. Sci. and Technol.* 48 (18), 10690–10698. doi:10.1021/es501655v
- Quik, J. T. K., van De Meent, D., and Koelmans, A. A. (2014b). Simplifying modeling of nanoparticle aggregation–sedimentation behavior in environmental systems: a theoretical analysis. *Water Res.* 62, 193–201. doi:10.1016/j.watres.2014.05.048
- Quik, J. T. K., Velzeboer, I., Wouterse, M., Koelmans, A. A., and Van de Meent, D. (2014a). Heteroaggregation and sedimentation rates for nanomaterials in natural waters. *Water Res.* 48, 269–279. doi:10.1016/j.watres.2013.09.036
- Ranjbari, K., Lee, W. L., Ansari, A., Barrios, A. C., Sharif, F., Islam, R., et al. (2022). Controlling silver release from antibacterial surface coatings on stainless steel for biofouling control. *Colloids Surfaces B Biointerfaces* 216, 112562. doi:10.1016/j.colsurfb.2022.112562
- Rearick, D. C., Telgmann, L., Hintelmann, H., Frost, P. C., and Xenopoulos, M. A. (2018). Spatial and temporal trends in the fate of silver nanoparticles in a whole-lake addition study. *PLoS One* 13 (8), e0201412. doi:10.1371/journal.pone.0201412
- Rong, H., Garg, S., Westerhoff, P., and Waite, T. D. (2018). *In vitro* characterization of reactive oxygen species (ROS) generation by the commercially available Mesosilver™ dietary supplement. *Environ. Sci. Nano* 5 (11), 2686–2698. doi:10.1039/c8en00701b
- Sharma, V. K., Siskova, K. M., Zboril, R., and Gardea-Torresdey, J. L. (2014). Organic-coated silver nanoparticles in biological and environmental conditions: fate, stability and toxicity. *Adv. Colloid Interface Sci.* 204, 15–34. doi:10.1016/j.cis.2013.12.002
- Song, Y., Rottschäfer, V., Vijver, M. G., and Peijnenburg, W. J. (2023). Developing and verifying a quantitative dissolution model for metal-bearing nanoparticles in aqueous media. *Environ. Sci. Nano* 10 (7), 1790–1799. doi:10.1039/d3en00096f
- Velzeboer, I., Quik, J. T. K., van de Meent, D., and Koelmans, A. A. (2014). Rapid settling of nanoparticles due to heteroaggregation with suspended sediment. *Environ. Toxicol. Chem.* 33 (8), 1766–1773. doi:10.1002/etc.2611
- Walters, C., Pool, E., and Somerset, V. (2013). Aggregation and dissolution of silver nanoparticles in a laboratory-based freshwater microcosm under simulated environmental conditions. *Toxicol. and Environ. Chem.* 95 (10), 1690–1701. doi:10.1080/02772248.2014.904141
- Wang, H., Adeleye, A. S., Huang, Y., Li, F., and Keller, A. A. (2015). Heteroaggregation of nanoparticles with biocolloids and geocolloids. *Adv. Colloid Interface Sci.* 226, 24–36. doi:10.1016/j.cis.2015.07.002
- Wimmer, A., Kalinnik, A., and Schuster, M. (2018). New insights into the formation of silver-based nanoparticles under natural and semi-natural conditions. *Water Res.* 141, 227–234. doi:10.1016/j.watres.2018.05.015
- Wimmer, A., Markus, A. A., and Schuster, M. (2019). Silver nanoparticle levels in river water: real environmental measurements and modeling approaches—a comparative study. *Environ. Sci. and Technol. Lett.* 6 (6), 353–358. doi:10.1021/acs.estlett.9b00211
- Wu, J., Sun, J., Bosker, T., Vijver, M. G., and Peijnenburg, W. J. (2023). Toxicokinetics and particle number-based trophic transfer of a metallic nanoparticle mixture in a terrestrial food chain. *Environ. Sci. and Technol.* 57 (7), 2792–2803. doi:10.1021/acs.est.2c07660
- Yin, Y., Liu, J., and Jiang, G. (2012). Sunlight-induced reduction of ionic Ag and Au to metallic nanoparticles by dissolved organic matter. *ACS nano* 6 (9), 7910–7919. doi:10.1021/nn302293r
- Zhang, W., Ke, S., Sun, C., Xu, X., Chen, J., and Yao, L. (2019). Fate and toxicity of silver nanoparticles in freshwater from laboratory to realistic environments: a review. *Environ. Sci. Pollut. Res.* 26, 7390–7404. doi:10.1007/s11356-019-04150-0